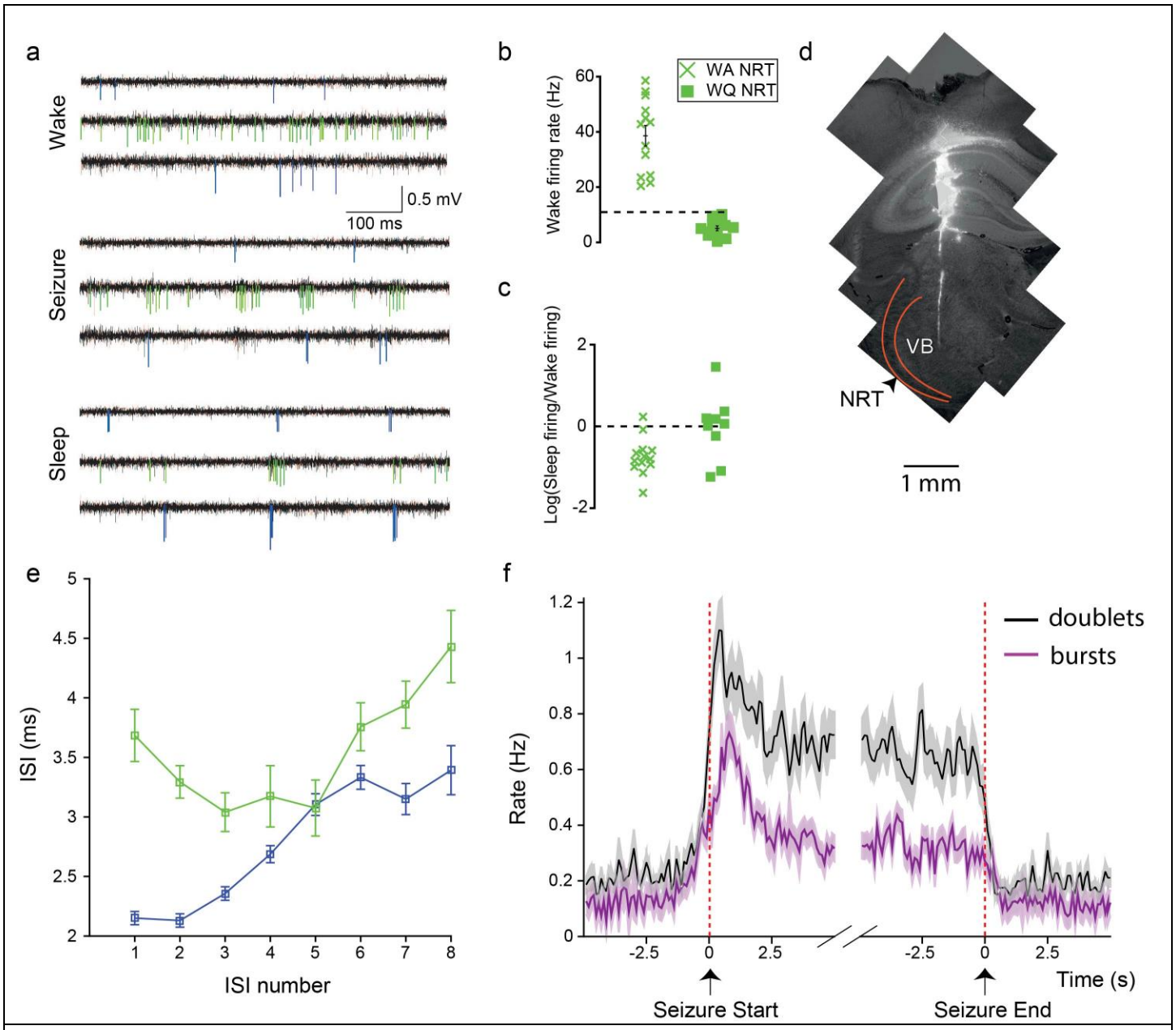

Supplementary Figure 1

Classification of action potentials of TC and NRT neurons.

(**a**) Example of high-pass filtered extracellular recording traces with TC (blue) and NRT (green) neuron action potentials recorded during periods of wakefulness (top), ASs (middle) and non-REM sleep (bottom) highlight the consistency of action potential sorting across different behavioral states and levels of synchrony. (**b**) Firing rate of all NRT neurons during wakefulness showing the demarcation between wake-active (WA, n=13) and wake-quiescent (WQ, n=9) NRT neurons at 10 Hz (dashed black line), as originally indicated by Halassa et al.

(Cell, 2014). Black lines are mean±SEM. (**c**) Log of the ratio of wake firing rate to sleep firing rate of NRT neurons, with all but one WA neuron having a negative value, confirms the presence of two NRT neuron groups with different firing rate during wakefulness. (**d**) Merged brightfield and TRITC-filtered images showing the final position of a silicone probe marked with Vybrant-Dil dye within the VB. Orange outlines indicate a portion of the NRT. (**e**) Burst signature of GAERS TC (blue) and NRT (green, both WA and WQ) neurons during non-REM sleep show their characteristic decelerando and accelerando-decelerando patterns, respectively (n=139 TC neurons; n=25 NRT neurons). Points are mean and error bars are ±SEM. (**f**) Temporal dynamics of the rate of occurrence of bursts containing ≥ 3 action potentials (purple line: mean; shaded areas: ±SEM) and action potential doublets (black) of GAERS TC neurons (n=124) before, during and after ASs. Note the strong qualitative similarities between the two firing types. Dashed red lines indicate times of start and end of SWDs in the EEG.

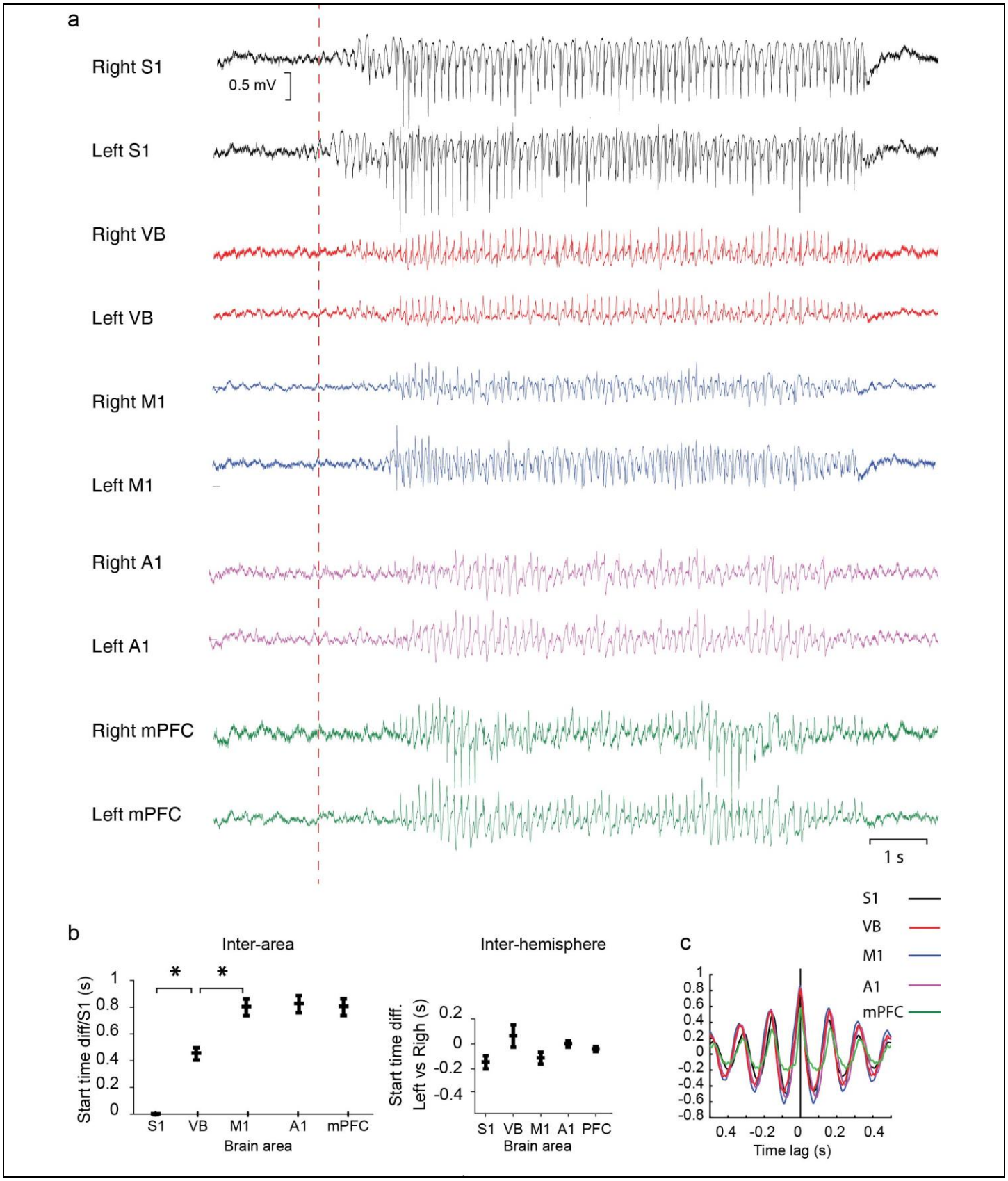
a
Right S1
0.5 mV
Left S1
Right VB
Left VB
Right M1
Left M1
Right A1
Left A1
Right mPFC
Left mPFC
1 s
b
Inter-area
Start time diff/S1 (s)
1
0.8
0.6
0.4
0.2
0
*
*
S1
VB
M1
A1
mPFC
Brain area
Inter-hemisphere
Start time diff.
Left vs Righ (s)
0.2
0
-0.2
-0.4
S1
VB
M1
A1
PFC
Brain area
c
S1
VB
M1
A1
mPFC
1
0.8
0.6
0.4
0.2
0
-0.2
-0.4
-0.6
-0.8
0.4
-0.2
0
0.2
0.4
Time lag (s)

Supplementary Figure 2
SWDs occur in cortical S1 earlier than in VB and other cortical regions of GAERS.
(**a**) EEG traces showing the start of a GAERS bilateral SWD in the perioral region of the primary somatosensory cortex (S1) before the ventrobasal thalamic nucleus (VB), the primary motor cortex (M1), the primary auditory cortex (A1) and the medial prefrontal cortex (mPFC). (**b**) Left: difference in the start time of SWDs between the recorded areas (the start of the SWDs in S1 is taken as time zero). Note the statistically significant delay in the start time between S1 ($p=8.1x10^{-17}$, n=41, two-sided Mann-Whitney U test) and VB, and between VB and the other cortical areas ($p=4.8x10^{-5}$, n=41, two-sided Mann-Whitney U test). Points are mean and error bars are ±SEM. Right: lack of any significant difference in the start of SWDs between the right and left hemisphere in the brain regions examined (p=0.9, 0.95, 0.89, 0.95 and 0.99, n=41, two-sided Mann-Whitney U test). Values are mean±SEM. (**c**) Superimposed cross-correlograms of SWC-spikes show no time-lag among left and right hemispheres for different brain regions (n= 41 SWDs in 3 GAERS for **b** and **c**).

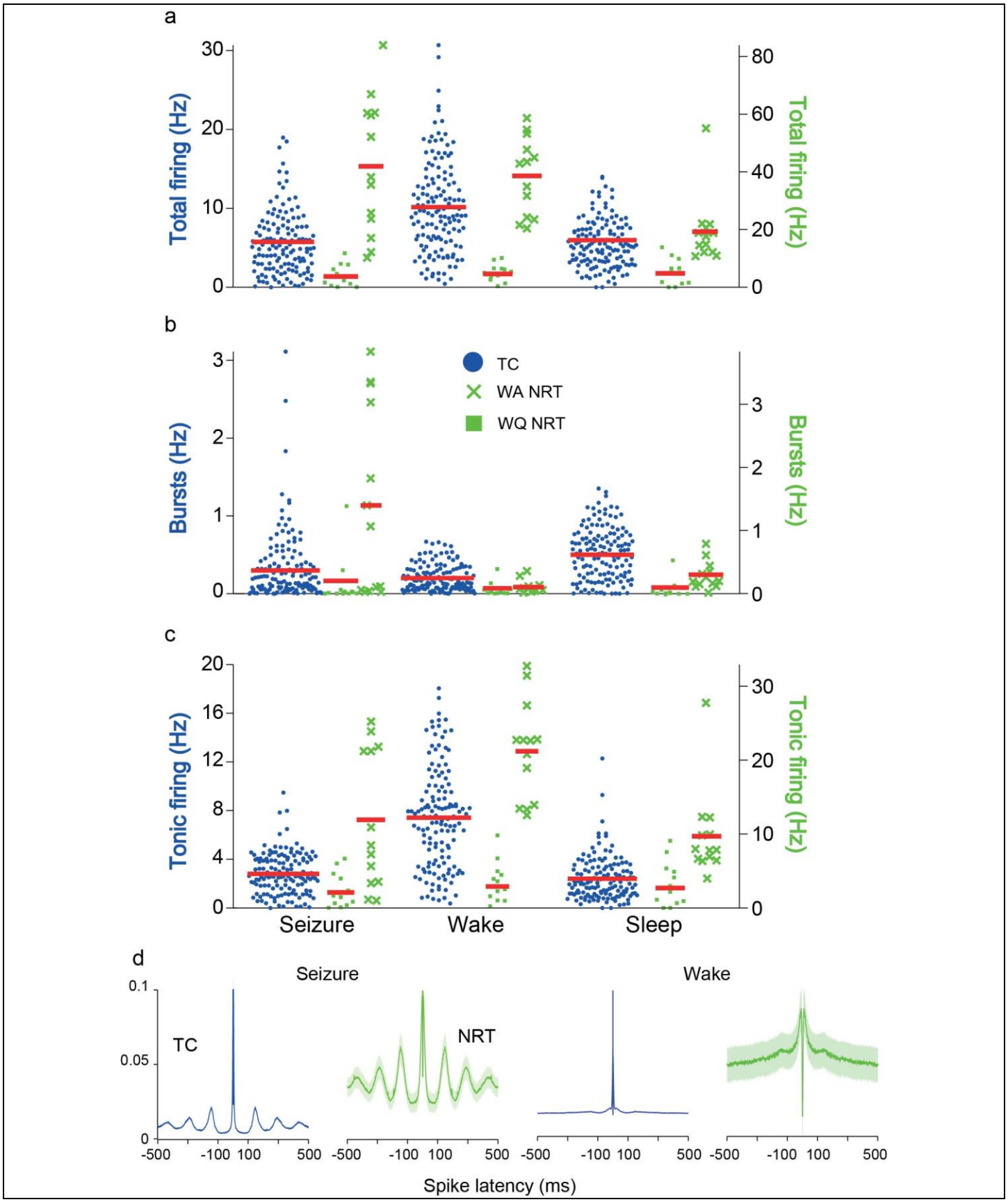
a
Total firing (Hz)
Total firing (Hz)
b
Bursts (Hz)
Bursts (Hz)
TC
WA NRT
WQ NRT
c
Tonic firing (Hz)
Tonic firing (Hz)
Seizure
Wake
Sleep
d
Seizure
Wake
TC
NRT
Spike latency (ms)

Supplementary Figure 3
Firing properties of GAERS TC and NRT neurons in different behavioral states.
(**a**,**b**,**c**) Rate of different firing types (total, bursts, tonic) of GAERS TC (blue, n=139) and NRT (wake-active, WA, n=13; wake-quiescent, WQ, n=12) neurons during ASs, wakefulness and non-REM sleep. Left and right axes refer to TC and NRT neurons, respectively. Horizontal red lines indicate mean (further data in Supplementary Table 1). (**d**) Autocorrelograms of GAERS TC (blue, n=139) and NRT (green, n=25) neuron firing during ASs (left) and wakefulness (right). Lines are mean and shaded areas are ±SEM.

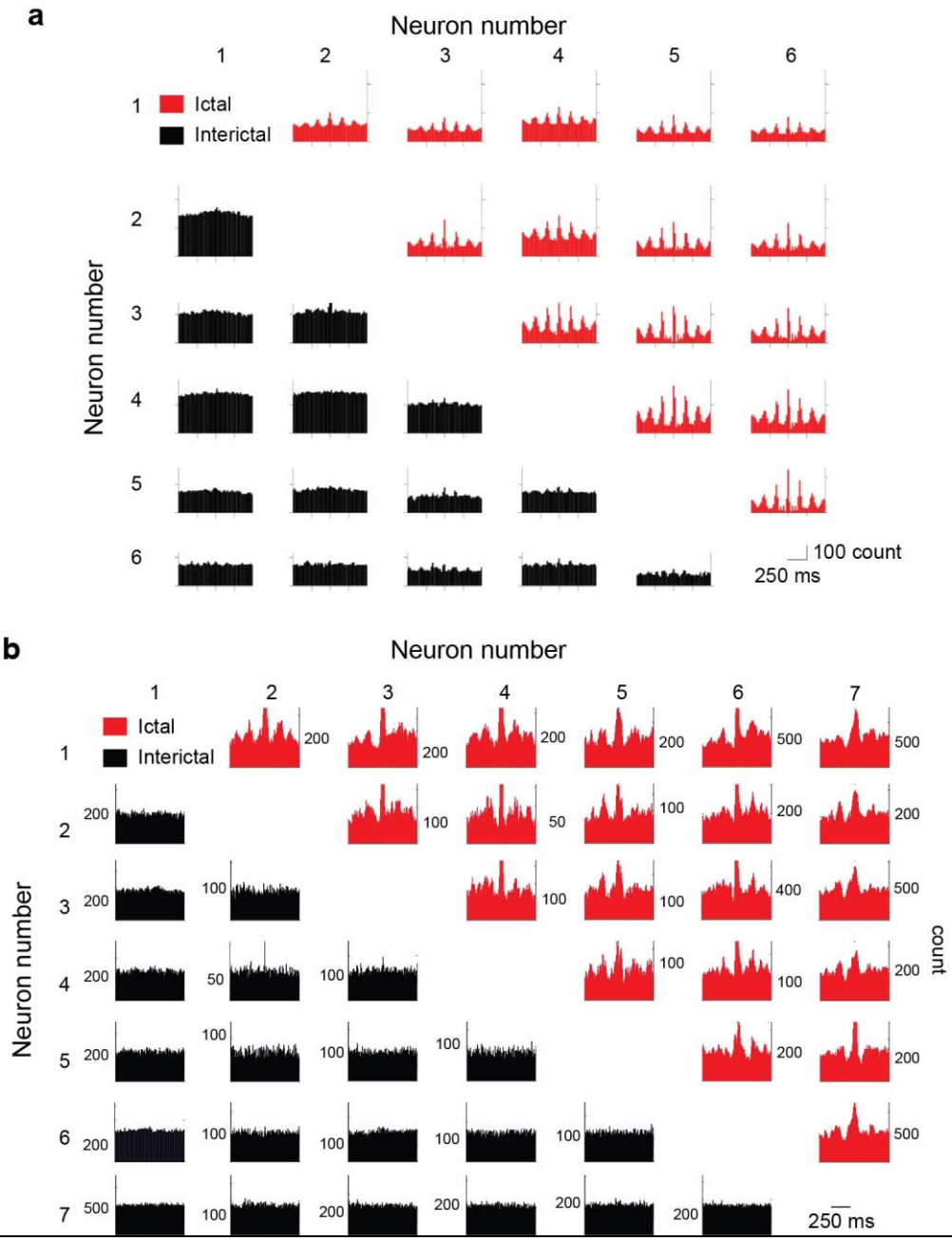

Supplementary Figure 4

Synchrony of thalamic neuron firing during ASs.

(**a**) Cross-correlograms of total firing of 6 simultaneously recorded GAERS TC neurons during interictal periods (black plots) and ASs (red plots). (**b**) Cross-correlograms of total firing of 7 simultaneously recorded WA NRT neurons during interictal periods (black plots) and GHB-elicited ASs (red plots) in a Wistar rat injected with 100 mg/kg i.p. of γ-butyrolactone, a GHB pro-drug (see Venzi et al., CNS Neurosci. Ther., 2015) (cf. Supplementary Fig. 7 and Online Methods).

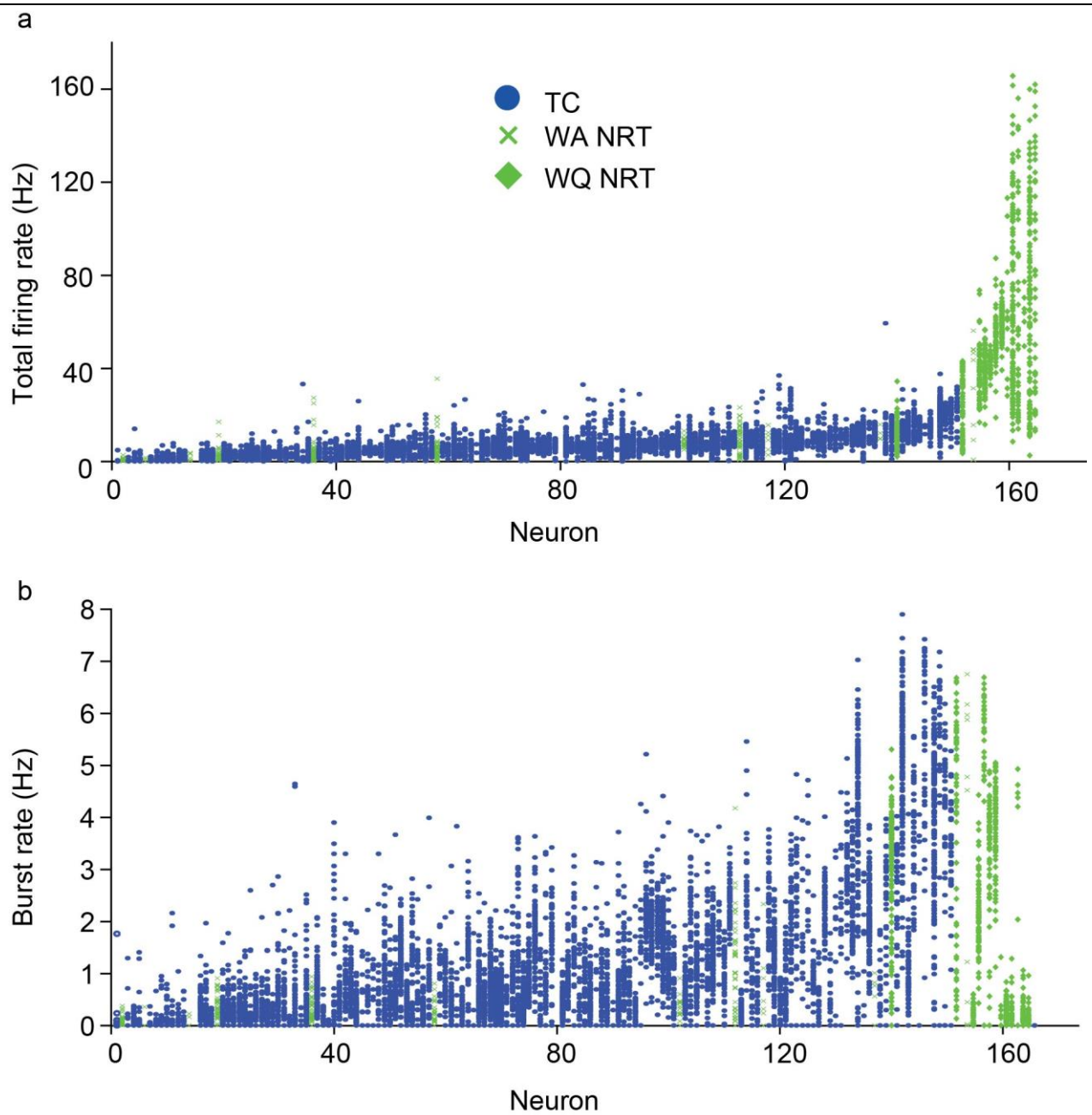

Supplementary Figure 5

Firing type and rate variation between ASs in GAERS.

Total (**a**) and burst (**b**) firing rate plotted individually for each AS and each TC (blue, n=139) and NRT (green, n=25) neuron, ranked on the x-axis from lowest to highest mean firing rate. The high variability for many neurons, and the absence of a bimodal distribution within individual neurons, indicate a large graduated range of neuronal behaviors during ASs in GAERS.

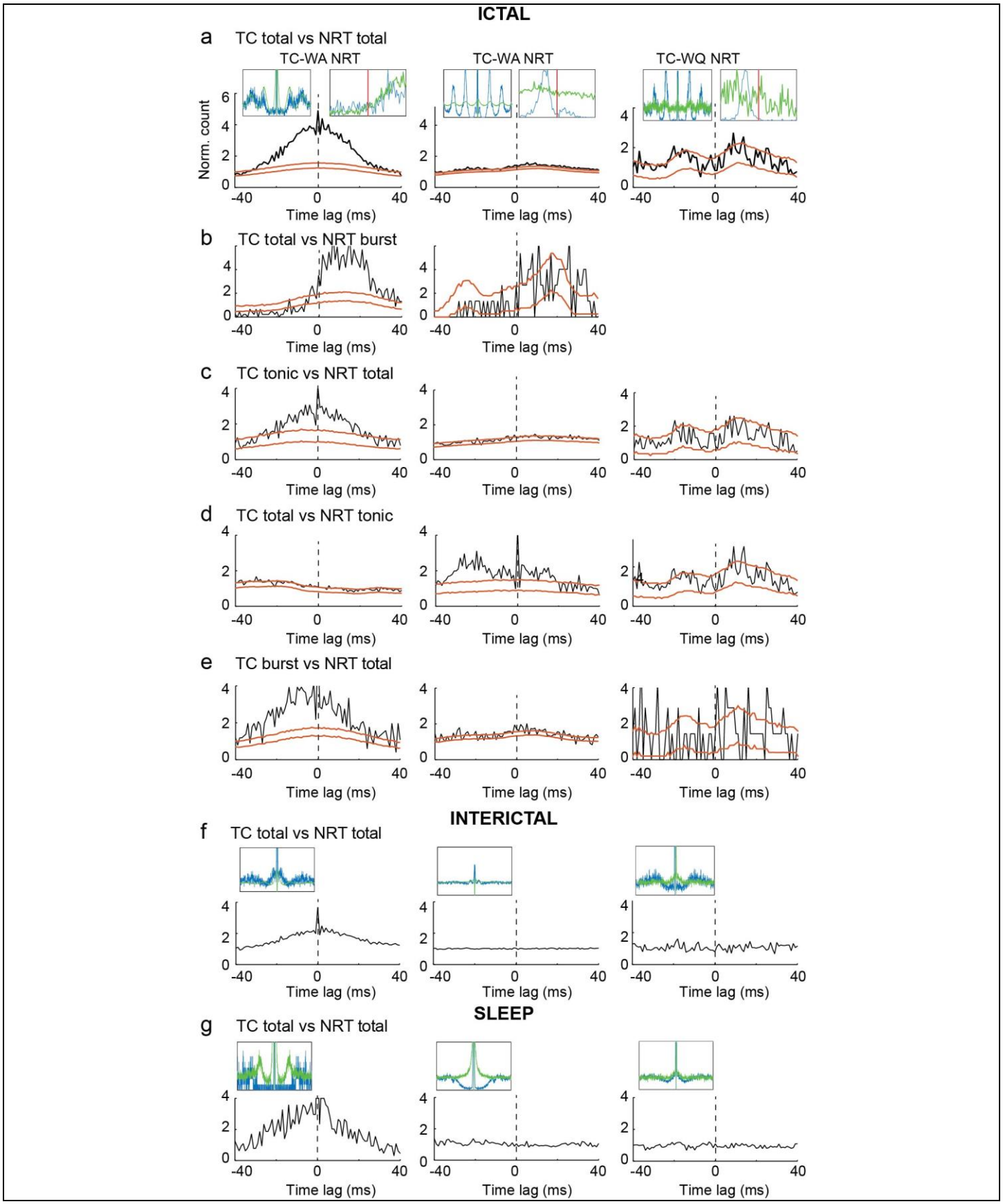
ICTAL
a
TC total vs NRT total
TC-WA NRT
TC-WA NRT
TC-WQ NRT
Norm. count
Time lag (ms)
b
TC total vs NRT burst
c
TC tonic vs NRT total
d
TC total vs NRT tonic
e
TC burst vs NRT total
INTERICTAL
f
TC total vs NRT total
SLEEP
g
TC total vs NRT total

Supplementary Figure 6
Different firing correlations between GAERS TC and NRT neuron pairs.
(**a**) Examples of ictal total firing XCors of a TC-WA NRT neuron pair with a symmetric peak centered on the SWC spike (left), a TC-WA NRT neuron pair with no peak or trough (middle), and a TC-WQ NRT neuron pair (right) from GAERS. Orange lines indicate confidence intervals of expected correlations (CI: 5%-95%) estimated from surrogate firing time for each neuron in its respective firing distribution relative to the SWC (Online Methods). Top left insets in (**a**,**f**,**g**) show superimposed autocorrelograms for the respective TC (blue) and NRT (green) neurons calculated between -400 and +400 ms (each curve maximum amplitude is normalized to 1). Top right insets in (**a**) show superimposed spike distribution of the respective TC (blue) and NRT (green) neuron calculated for the time period -40 to +40 ms with respect to the SWC spike. (**b**-**g**) XCors of the same pairs as in (**a**) for different types of firing (as indicated) during ASs (**b**-**e**), awake interictal periods (**f**) and non-REM sleep (**g**).

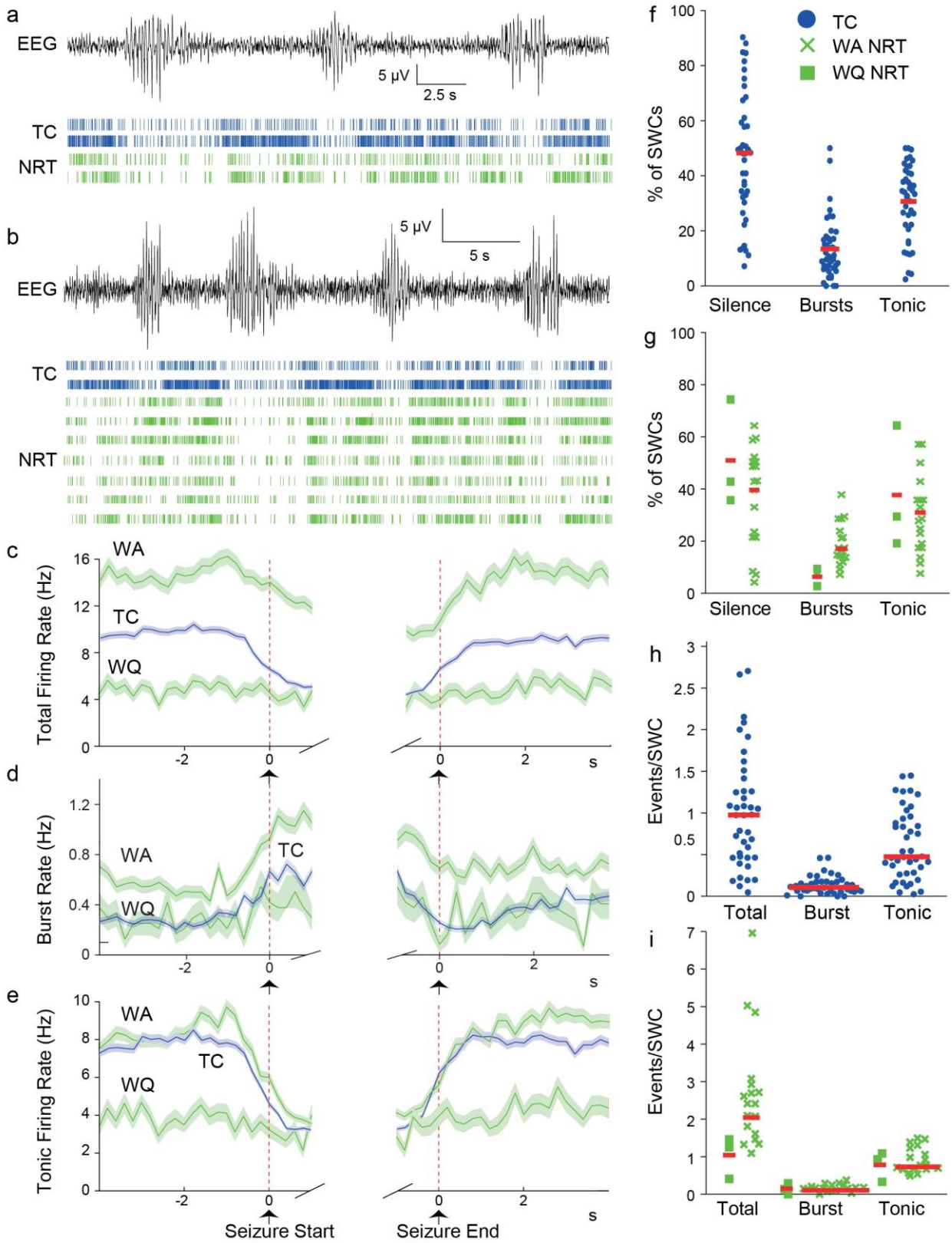

Supplementary Figure 7

Temporal dynamics of TC and NRT neuron firing in the GHB model.
In 3 Wistar rats injected with 100 mg/kg i.p. of γ-butyrolactone, a GHB pro-drug (Online Methods), we recorded 39 TC neurons, 18 WA and 3 WQ NRT neurons during 332 ASs that had a duration of 3.03±1.08 s and a SWD frequency of 5.09±0.85 Hz. (**a**) Spike-time raster plots (bottom traces) from 2 TC (blue) and 2 WA NRT (green) neurons with time-matched EEG (top trace) during GHB-elicited ASs. (**b**) Same as in (**a**) for 2 TC (blue) and 7 WA NRT (green) neurons from another GBL-injected Wistar rat. Note the sparse firing of TC and WA NRT neurons during ASs. (**c**,**d**,**e**) Temporal evolution of different firing types before, during and after GHB-elicited ASs for 39 TC (blue) and NRT (green) neurons (n=18 WA and 3 WQ) (lines: mean, shaded areas: ±SEM). Red dashed lines indicate the start and end of ASs. Note that the ictal firing dynamics of TC neurons during these seizures were remarkably similar to those observed during spontaneous ASs in GAERS, in particular i) the marked ictal decrease in total and tonic firing (52% and 55%, respectively), ii) the low burst rate (0.1 burst/SWC) and iii) the average ictal total firing (0.94 spike/SWC) (Supplementary Table 1). However, the sharp peak in burst firing observed within the first second of the ictal activity in GAERS was absent in the GHB model. WA NRT neurons had overall ictal activity profiles similar to GAERS WA NRT neurons, with two notable exceptions: i) total firing exhibited a 26% decrease ictally compared to interictally, and ii) burst firing increased monotonically without a peak around the interictal-to-ictal transition. Notwithstanding the decrease in ictal total firing, there was a consistent output of the NRT population during ASs as indicated by the peaks in the XCors between simultaneously recorded NRT neurons (Supplementary Fig. 4b). Notably, the mean interictal rate of different firing types of TC and particularly of WA-NRT neurons was on average lower in the GHB model than the respective rates in GAERS (cf. Fig. 2), probably as a result of GHB-induced sedation (see Venzi et al., CNS Neurosci. Ther., 2015). (**f**,**g**) Percentage of SWCs accompanied by electrical silence, bursts and tonic single action potentials for TC neurons (**f**), WA and WQ NRT neurons (**g**). (**h**,**i**) Events of each firing type per SWC in TC (**h**) and NRT (**i**) neurons. Red lines in (**f**-**i**) indicate mean values. As in GAERS, WQ-NRT neurons in the GHB model did not show any significant AS-associated variation in firing or any significant AS-linked feature in subsequent analyses.

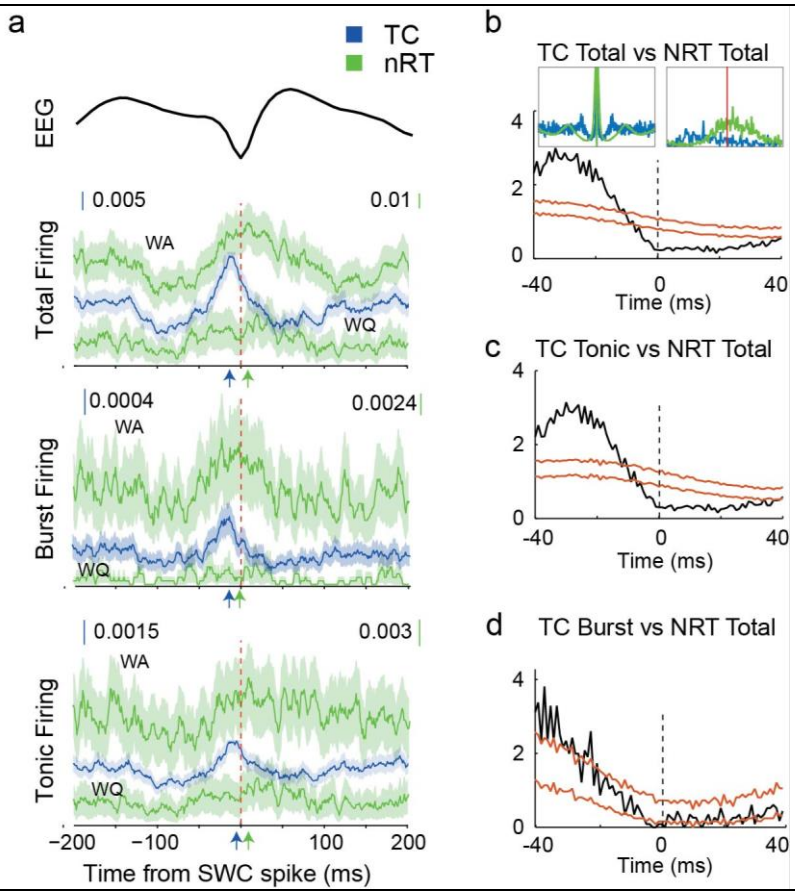

Supplementary Figure 8

Synchrony of TC and NRT neuron ictal firing in the GHB model.

(**a**) SWC-spike-triggered averages (lines: mean; shaded areas: ±SEM) of total, burst and tonic firing for GHB TC (n=44), and WA (n=18) and WQ (n=3) NRT neurons. Note the different peak time (color coded arrows) of TC and WA NRT neurons relative to SWC spike (red vertical line) and the strong temporal overlap between the ascending phase of the curves of the two thalamic populations. Ictal burst and tonic firing peaks had similar shape and latency (to the SWC-spike) to those of total firing (Supplementary Table 2). No clear peaks are evident for WQ NRT neurons. (**b**) Typical examples of ictal firing XCors of a TC-WA NRT neuron pair recorded during GBL-elicited ASs. Orange lines indicate confidence intervals (5-95%) of expected correlations estimated as in Fig. 5 (Online Methods). Thirty-two pairs of simultaneously recorded TC and NRT neuron pairs had broad peaks before time-zero indicating an increased probability of NRT neurons to fire after TC neurons. Note the presence of a significant trough when TC neuron total and tonic firing **(b,c)**, but not burst firing **(d)**, are used for the XCors, a result similar to that in GAERS. Top left inset in (**b**) shows superimposed autocorrelograms for the respective TC (blue) and NRT (green) neurons calculated between -400 and +400 ms.

Top right inset in (**b**) shows superimposed spike distribution of the respective TC (blue) and NRT (green) neuron calculated for the time period -40 to +40 ms with respect to the SWC-spike.

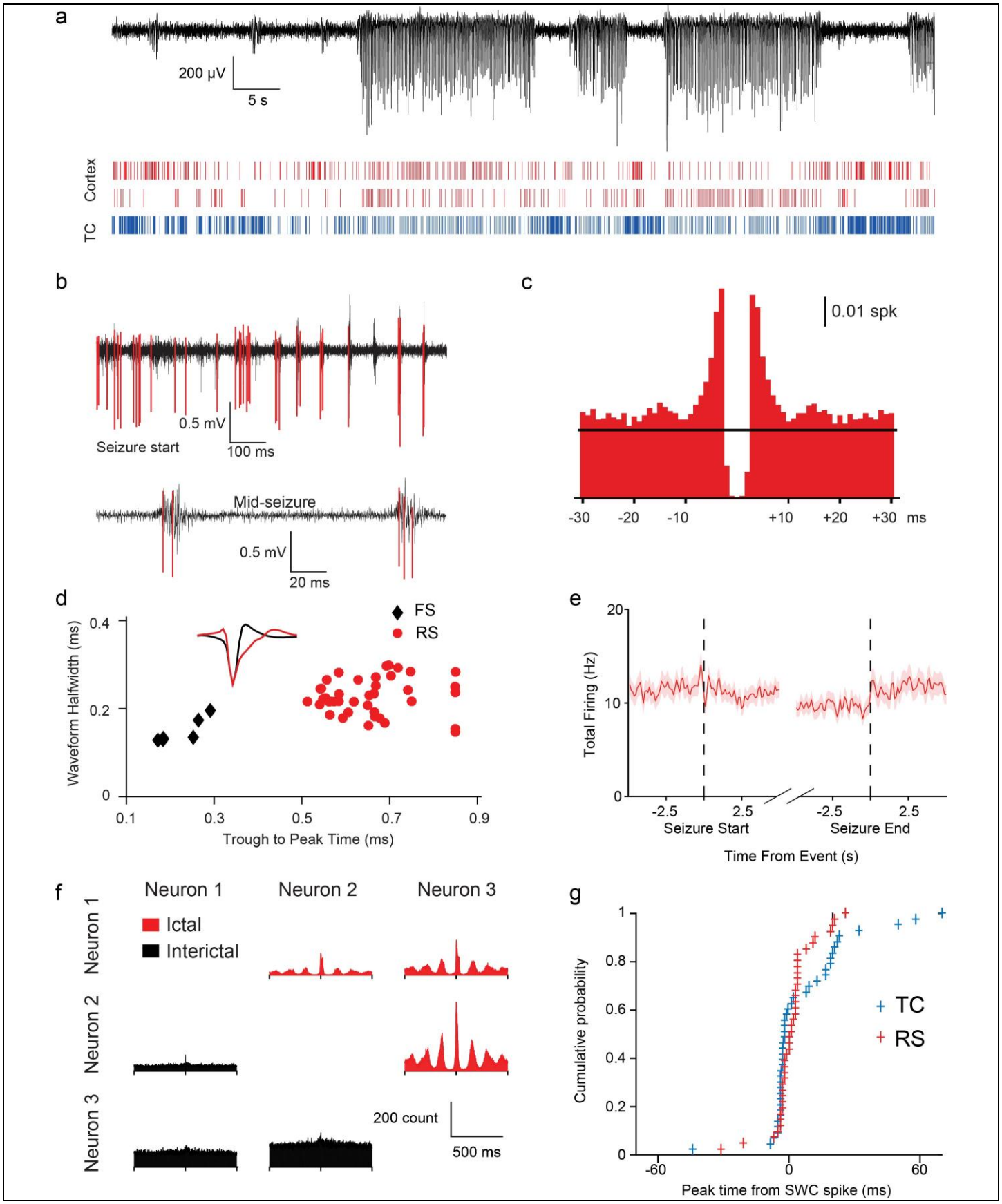
a
200 µV
5 s
Cortex
TC
b
0.5 mV
Seizure start
100 ms
Mid-seizure
0.5 mV
20 ms
c
0.01 spk
-30
-20
-10
+10
+20
+30
ms
d
FS
RS
Waveform Halfwidth (ms)
0.4
0.2
0
0.1
0.3
0.5
0.7
0.9
Trough to Peak Time (ms)
e
Total Firing (Hz)
20
10
0
-2.5
2.5
Seizure Start
Seizure End
Time From Event (s)
f
Neuron 1
Neuron 2
Neuron 3
Ictal
Interictal
200 count
500 ms
g
Cumulative probability
1
0.8
0.6
0.4
0.2
0
-60
0
60
TC
RS
Peak time from SWC spike (ms)

Supplementary Figure 9
Action potential classification and firing dynamics of GAERS cortical putative excitatory neurons.
(**a**) EEG trace (top) and raster plots (bottom) showing SWDs and firing times, respectively, of simultaneously recorded single cortical and TC neurons. (**b**) High-pass filtered traces showing typical isolated cortical action potentials. (**c**) Auto-correlogram of a putative excitatory cortical neuron. (**d**) Action potential half-widths vs trough-to-peak times for putative inhibitory (n=5) (black, FS for fast-spiking) and excitatory (n=41) (red, RS for regular spiking) cortical neurons. Average action potential waveforms are shown in the inset. (**e**) Total firing rate of all cortical pyramidal neurons (n=41). Horizontal dashed line indicates the start and end of SWDs in the EEG. Lines are mean and shaded areas are ±SEM. (**f**) XCors of total firing of 3 simultaneously recorded cortical excitatory neurons during interictal periods (black) and ASs (red). (**g**) Cumulative distributions of the peak of total firing for all simultaneously recorded cortical excitatory (n=41) and TC (n=43) neurons show no difference between the two neuronal populations (p=0.4892, Kolmogorov-Smirnov test).

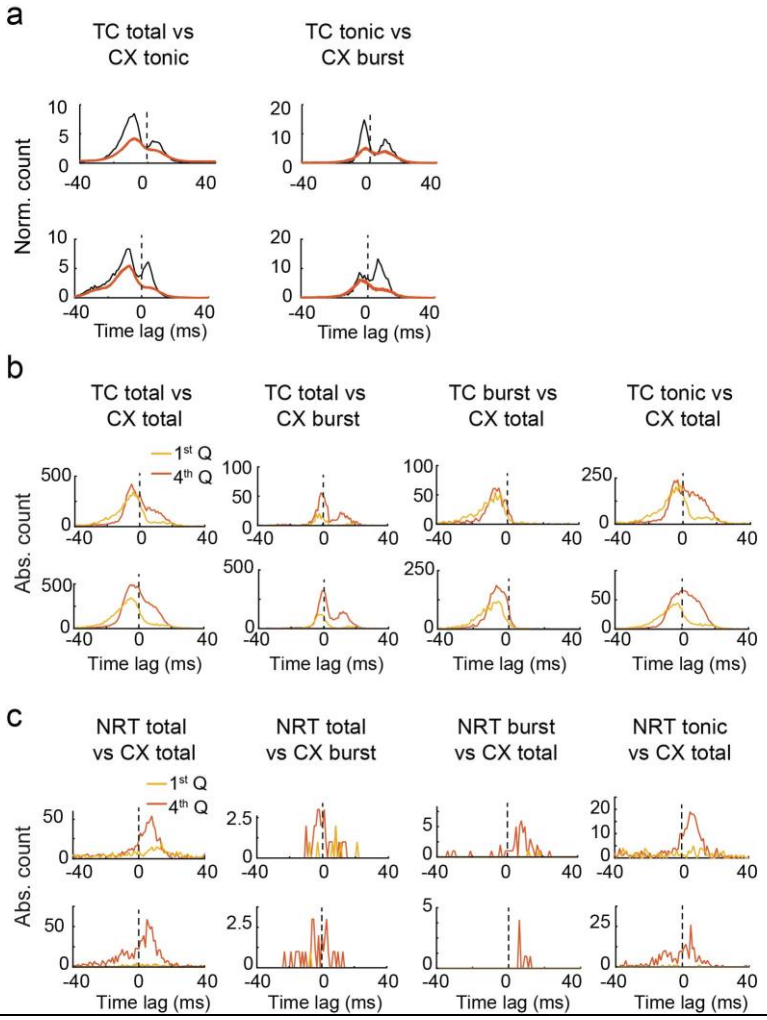

Supplementary Figure 10

Firing-mode specific, cortico-thalamic interactions in GAERS for SWC-spikes of different amplitude.

(**a**) XCors of different firing types (TC total and CX tonic) and (TC tonic and CX burst) for the same TC and cortical (CX) neuron pairs shown in Fig. 6a. (**b**) XCors of different types of TC and CX neuron firing (same pairs as in Fig. 6a) for SWC-spikes of largest (4th quartile, orange line) or smallest (1st quartile, yellow line) amplitude. (**c**) Same as in (**b**) for the same pairs of NRT and CX neurons as in Fig. 6b.

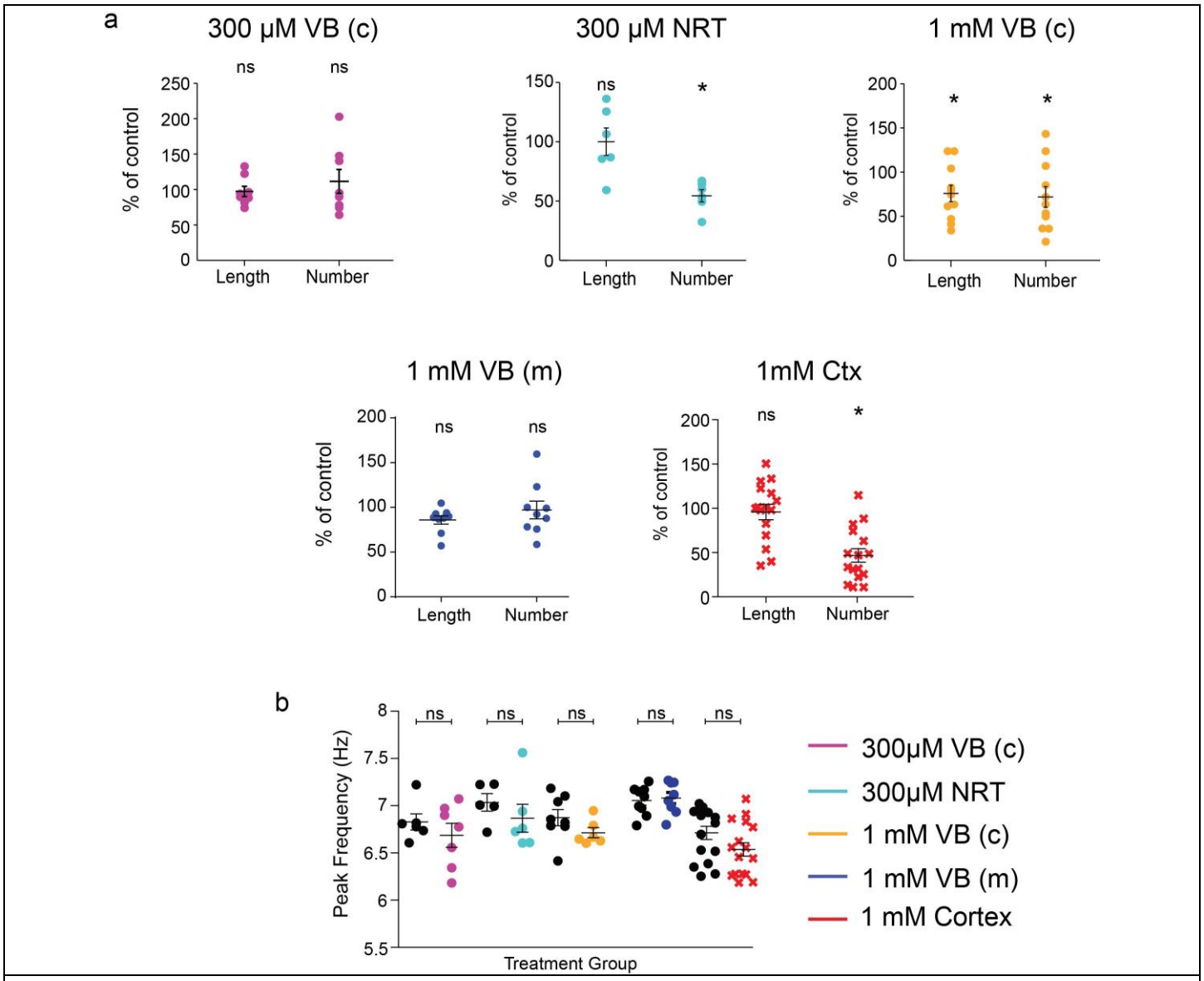

Supplementary Figure 11

Effect of bilateral microdialysis application of TTA-P2 on the number and duration of ASs in GAERS.

(**a**) Each plot show the effect of TTA-P2 applied in the indicated brain regions (c and m indicate central to the VB and medial to the VB, respectively) on the mean number of ASs and mean length of individual seizures (from left to right and top to bottom: n=7, 6, 10, 9, and 16 animals, p=0.742, 0.547, 1, 0.031, 0.014, 0.024, 1, 0.313, 0.433, 0.013, paired two-sided Wilcoxon signed-rank test). (**b**) Effect of TTA-P2 applied in the indicated brain regions on the mean peak frequency of SWDs for the same groups of animals, compared to vehicle microdialysis application (from left to right: n=7, 6, 7, 8, and 16 animals, p=0.563, 0.438, 0.625, 0.945, 0.025, paired two-sided Wilcoxon signed-rank test). In all subfigures, black lines are mean and error bars are ±SEM.

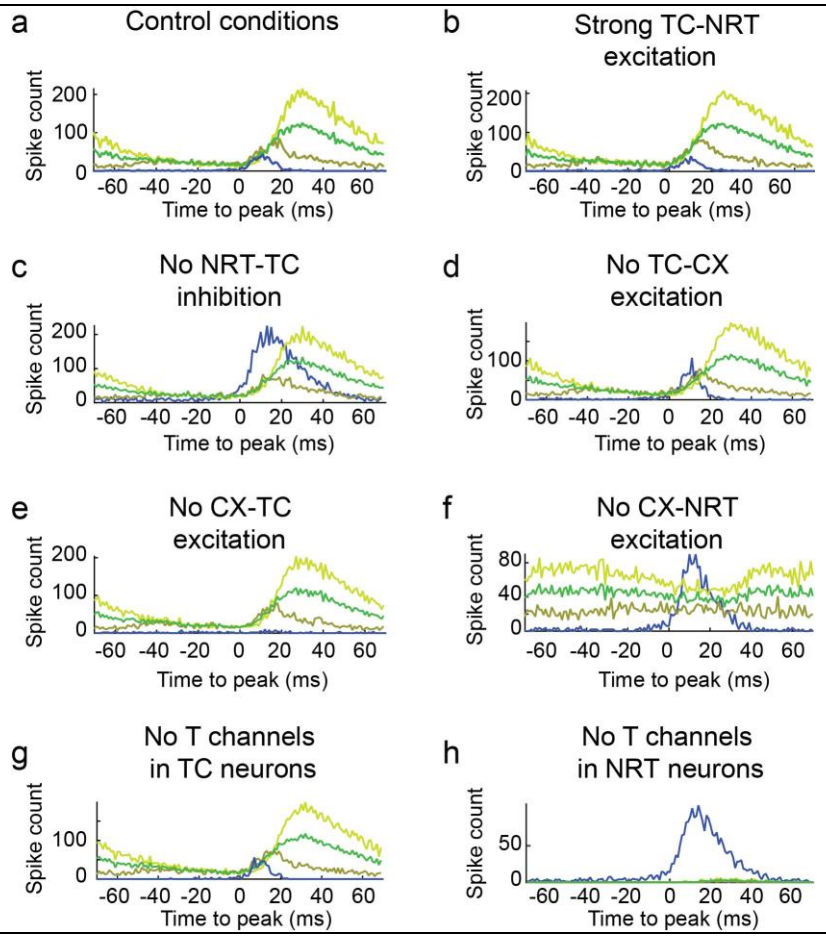

Supplementary Figure 12

Firing distribution of TC and NRT neurons in the cortico-thalamic model.

(**a**-**h**) Each panel shows the firing distribution of simulated activity in TC (blue) and NRT (light green depolarized, brown hyperpolarized, dark green mean of both) neurons of the cortico-thalamic model during repetitive sequences of trains of 5 EPSPs delivered to the cortical neurons at 7 Hz to mimic the GAERS SWD frequency. Time-zero is that of the 3rd EPSP in each stimulation train (cf. Fig. 8).